Macromolecular Rapid Communications
www.mrc-journal.de

Check for updates

Creating Transient Gradients in Supramolecular Hydrogels

*Lisa Thomson, Ralf Schweins, Emily R. Draper, and Dave J. Adams**

The self-assembly of low molecular weight gelators in water usually produces homogeneous hydrogels. However, homogeneous gels are not always desired. Using a photoacid generator, it is shown how to form gels with a transient gradient in stiffness, proved using cavitation and bulk rheology. Small-angle neutron scattering is used to show that the gels formed by photoacid are the result of the same structures as when using a conventional pH trigger. Patterned gels can also be formed, again with transient differences in stiffness.

Supramolecular hydrogels are formed by trapping water within a network.[1] The network consists of low molecular weight gelators that self-assemble when a stimulus is applied. Such networks are held together through physical cross-links created by weak, non-covalent interactions such as hydrogen bonds, hydrophobic interactions, and π–π stacking and so generally result in reversible gels.[2,3] As the networks are formed via self-assembly, it can be hard to control how the fibers form and cross-link. Hence, it can be difficult to spatially control the gel networks, which requires that we can direct assembly over the various length scales associated with a network.[4]

Preparing gels with a gradient in properties has potential uses, with controlled heterogeneity leading to many possible applications, including in tissue engineering where there can be a benefit from forming gels with a gradient of stiffness, mimicking the various tissue stiffnesses present in the body.[5] Different organs and tissues vary in stiffness, as do cancerous tissues which are stiffer than healthy tissue.[5d,e] Varying stiffness also affects cell adhesion and morphology.[5d]

A number of methods have been developed to prepare gels with gradients of properties, including gradients of stiffness[5c,d] and of concentration.[6] A common method is to use light to control gelation and form gradients.[7] For example, Murata et al. used a cholesterol-based gelator, which could be cycled between the *cis-* and *trans*-isomers using light. Since the *trans*-form formed gels while the *cis*-isomer did not, cycling between the isomers allowed sol-to-gel-to-sol transitions. By introducing a template and selectively gelling only part of a system, reversible patterns were created, showing spatially-controlled gel formation.[7a] Photomasks and light can also be used to form gradual gradients.[5d] By slowly moving the photomask while irradiating, different gradients in stiffness of an acrylamide/bis-acrylamide gel could be achieved. Other work focusses on using microfluidic channels to form gradients.[8]

Although gradients have been formed within gels, there is generally little discussion as to the timescale over which these gradients persist. There are a few exceptions. When forming gels with a concentration gradient, Karpiak et al. noted a time dependence; the initial gradient in concentration created within the gel became more continuous and gradual, instead of having disjointed layers, attributed to diffusion between layers.[9] A similar effect was shown when proton diffusion was used to form gels using an acid-triggered gel.[10] By adding drops of acid to one side of a cell containing the gelator solution at high pH and a pH indicator, it was possible to see the change in pH as the acid diffused through the cell.

We focus here on gels formed by the self-assembly of a functionalized dipeptide (diphenylalanine conjugated at the N-terminus to a naphthalene moiety, 2NapFF, **Figure 1**a). As described previously, 2NapFF forms homogeneous gels when an acid is added to a solution of 2NapFF at high pH and gels at low pH.[11] Anticipating the need for restricted diffusion in this work, we chose 2NapFF on the basis of the formation of the persistent micelles at high pH. The hydrolysis of glucono-δ-lactone (GdL) to gluconic acid is an effective method of forming homogeneous gels with gelators such as 2NapFF.[12] For this gelator, micellar structures are formed at high pH.[11b] These are protonated as the pH is lowered, resulting in a network of fibers.[11b]

Photoacid generators (PAGs) can also be used to lower the pH. While PAGs have been used to form gels with related dipeptides, the use of diphenyliodonium nitrate as a PAG to trigger gelation of a solution 2NapFF was unsuccessful.[13] Here, we show that the PAG 2-(4-methoxystyryl)-4,6-bis(trichloromethyl)-1,3,5-triazine (MBTT)[14] can be used to form gels with 2NapFF with controllable transient gradients in stiffness.

Initially, we focus on the homogeneous gels formed with GdL (Figure 1b). Since GdL is mixed with the solution and dissolves before hydrolysis occurs, a uniform pH change occurs to give homogeneous gels as we have described previously.[12]

L. Thomson, Dr. E. R. Draper, Prof. D. J. Adams
School of Chemistry
University of Glasgow
Glasgow G12 8QQ, Scotland
E-mail: dave.adams@glasgow.ac.uk

Dr. R. Schweins
Large Scale Structures Group
Institut Laue-Langevin
71 Avenue des Martyrs, CS 20156, 38042 GRENOBLE, Cedex 9, France

The ORCID identification number(s) for the author(s) of this article can be found under https://doi.org/10.1002/marc.202000093.

© 2020 The Authors. Published by WILEY-VCH Verlag GmbH & Co. KGaA, Weinheim. This is an open access article under the terms of the Creative Commons Attribution License, which permits use, distribution and reproduction in any medium, provided the original work is properly cited.

DOI: 10.1002/marc.202000093

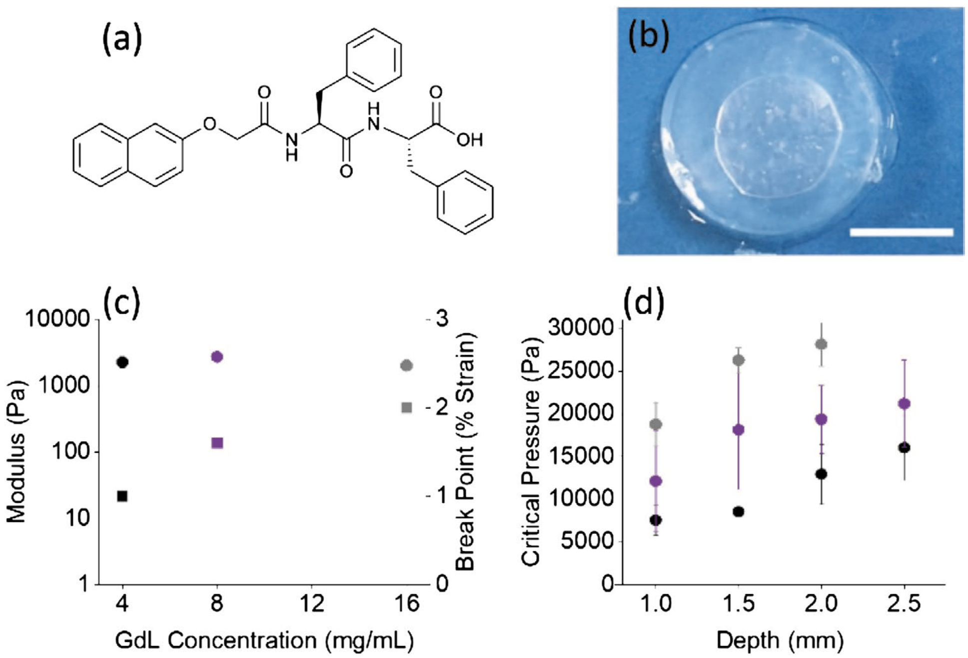

Figure 1. a) Structure of 2NapFF; b) GdL-triggered 2NapFF gel. An air bubble can be seen underneath the gel, formed when moving the gel onto a microscope slide for imaging. Scale bar represents 1 cm; c) bulk rheology (storage modulus shown by circles, and break point shown by squares) and d) cavitation rheology of gels formed using various GdL concentrations: 4 mg mL^{-1} GdL (black), 8 mg mL^{-1} GdL (purple), and 16 mg mL^{-1} GdL (grey). Error bars show the standard deviation between the samples, except for break point which does not have error bars. For the data in (c), the error bars are smaller than the data points. Measurements were performed in triplicate.

GdL concentrations of 4, 8, and 16 mg mL^{-1} were used to create 2NapFF gels which were analyzed using bulk rheology and cavitation rheology, a localized technique which can probe homogeneous and heterogeneous material at localized points in their native environments.[15] Here, an air bubble develops within the gel and the mechanical properties can be probed by the pressure that can be withstood before failure. The bulk rheology data for gels formed using GdL are very similar (Figure 1c), with no appreciable difference in stiffness or strength when using different concentrations of GdL. This is consistent with previous results.[16] Varying the concentration of GdL varies the kinetics of gelation with higher concentrations of GdL resulting in gels more quickly. However, the final G′ and G″ values obtained from bulk rheology are similar.[16,17] There were small changes in the strain at which the gels break, with the gels becoming slightly stronger as the concentration of GdL increased.

Cavitation rheology (Figure 1d) allows us to compare the rheological data at points within the same gel and hence determine gel homogeneity.[15a,c] We used cavitation rheology to probe the gels at different depths. As expected from our previous work on dipeptide gels using cavitation rheology,[15c] the critical pressure increases linearly with depth for these gels. Increasing the amount of GdL in the system results in a decrease in the final pH (Table S1, Supporting Information) and an increase in the critical pressure values at each needle depth. For gels prepared with 16 mg mL^{-1} GdL, no data could be collected at 2.5 mm as the critical pressure values were greater than our cavitation rheometer could measure (above 30 000 Pa). The constant values for the bulk rheology but increasing values for the cavitation rheology can be explained by the differences in length scale that are being probed. Cavitation rheology measures more local properties compared to bulk rheology and so these data imply that there are differences at this length scale that average out when the bulk rheology is measured. The critical pressures can be related to cavitation modulus and to those measured by rheology as described elsewhere,[15] but the key points we focus on here are best seen from the differences in trend as opposed to focusing on absolute values.

We then moved to using the PAG MBTT to decrease the pH. Adding the PAG as a hydrophobic additive to a solution of 2NapFF at high pH might be expected to interact with or affect the self-assembly of the dipeptide. Indeed, at high pH, the addition of MBTT induces a structural change compared to 2NapFF[11b] alone as shown by small-angle neutron scattering. Hollow tubes are formed at high pH, with a lower radius than the hollow tubes formed by 2NapFF alone.[11b] This shows that the presence of the hydrophobic additive affects the molecular packing at high pH, presumably by being incorporated into the micellar structures at high pH. However, on decreasing the pH, there is no difference in structure when 2NapFF is gelled by using the PAG and UV irradiation or by GdL. In both cases, the data could be fitted to an elliptical cylinder combined with a power law to take into account the scattering at low Q (the scattering vector) (Figure S10 and Table S2, Supporting Information). It is possible that the decomposition products from irradiation of the photoacid[14] could conceptually react with the 2NapFF. We have no data to suggest that this is the case and note that the similarity in structures in the gel state when gelled using GdL or the photoacid implies that this does not occur. The structural change induced by adding the PAG also results in a slight change in the apparent pK_a of the 2NapFF (Figure S11, Supporting Information).

 © 2020 The Authors. Published by WILEY-VCH Verlag GmbH & Co. KGaA, Weinheim

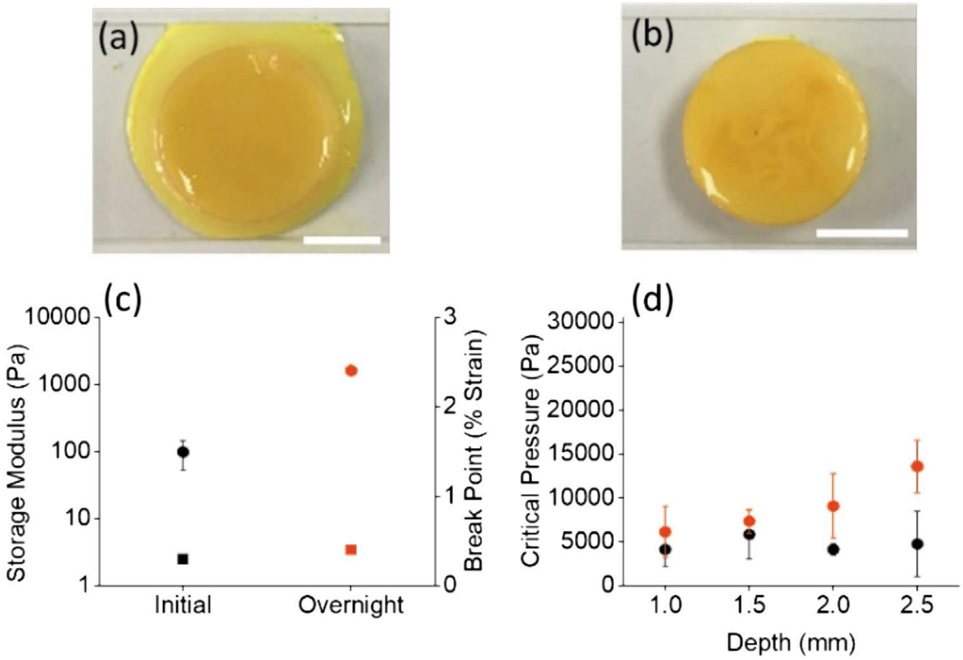

Figure 2. a) Picture of MBTT gel removed straight away from its mold after 6 h UV exposure. Since the gel is very weak at the bottom at this point, some damage occurs on removal from the mold and hence the liquid around the gel; b) Picture of MBTT gel kept in its mold overnight and removed the day following 6 h UV exposure. Scale bars represent 1 cm. c) Bulk (storage modulus shown by circles, and break point shown by squares) and d) cavitation rheology of gels formed using MBTT and 6 h of UV exposure. Black data points represent measurements taken straight after UV exposure and red data points represent measurements taken the day following UV exposure. Error bars show the standard deviation between the samples, except for break point which does not have error bars. Measurements were performed in triplicate.

Irradiating a solution of the 2NapFF containing MBTT at 365 nm resulted in a change in the pH and triggers gelation. We optimized the system (Figure S12, Supporting Information) such that 1.5 molar equivalents of MBTT were used as relative to 2NapFF. Irradiation for 4 h or longer resulted in gel formation. The gels were formed in molds, and at least 6 h irradiation was required to be able to form gels of sufficient robustness to be removed from the mold. Even at 6 h, removal from the mold caused some damage (**Figure 2**a). The weaker gels could however still be probed via cavitation rheology without removing from the mold.

Compared to the gels formed with GdL, the cavitation rheology shows a different trend for the gels formed with the PAG. Gels formed after 4 h of irradiation show a decreasing critical pressure with increasing needle depth using cavitation rheology (Figure S13, Supporting Information). These data can be explained by the formation of a gradient within the gel. The gels are formed by irradiation from the top. Hence, the change in pH, and therefore gelation, will begin at the top of the gel, with the bottom of the sample receiving less irradiation and hence will not reach such a low pH. We note that determining the percentage of the 2NapFF that is assembled into fibers and gel network as opposed to in the micellar aggregates is very difficult. Even NMR spectroscopy of the micellar aggregates at high pH (where the 2NapFF is most mobile) can only detect around 20% of the expected value[11] due to the persistence time in the micelles.

At longer irradiation times, for example, 6 h (Figure 2), the critical pressure values as measured by cavitation rheology remain relatively constant when increasing needle depth. A homogeneous gel would show an increase in the critical pressure with depth as for the GdL gels (see above), so these data show again that there is a gradient within the gel. These gels are however stiffer than those formed after 4 h of irradiation. After 7 or 8 h of irradiation (Figures S15 and S16, Supporting Information), the cavitation rheology data are similar to that for the homogeneous GdL gels, with critical pressure increasing with increasing needle depth. The critical pressures measured for the gels after 8 h irradiation are greater than those for the gel formed after 7 h. In all cases, we assume that the gradient is a result of light penetration as opposed to an inhomogeneous distribution of PAG throughout the sample; no gradient in the color is observed pre-gelation for example, which would be expected if mixing were non-uniform.

Interestingly, there is an aging effect. The data described above are for measurements on gels immediately after the cessation of irradiation. If the gels formed after 6–8 h of irradiation are allowed to stand overnight before being measured, the gels show data similar to that for the homogenous GdL gels, with the critical pressure increasing with depth. The gradients of stiffness produced are therefore only temporary, with proton diffusion leading to an equilibration in pH overnight and hence the initial gradient is lost (Table S3, Supporting Information).

Using a combination of both GdL and MBTT, it is possible to photopattern gels. We consider a photo-patterned gel as a gradient gel with a steep gradient between the photo-patterned sections. Previous work has described photo-patterning of multicomponent systems,[18] whereby either one or both components are induced to gel. Here, we show photo-patterning using only

© 2020 The Authors. Published by WILEY-VCH Verlag GmbH & Co. KGaA, Weinheim

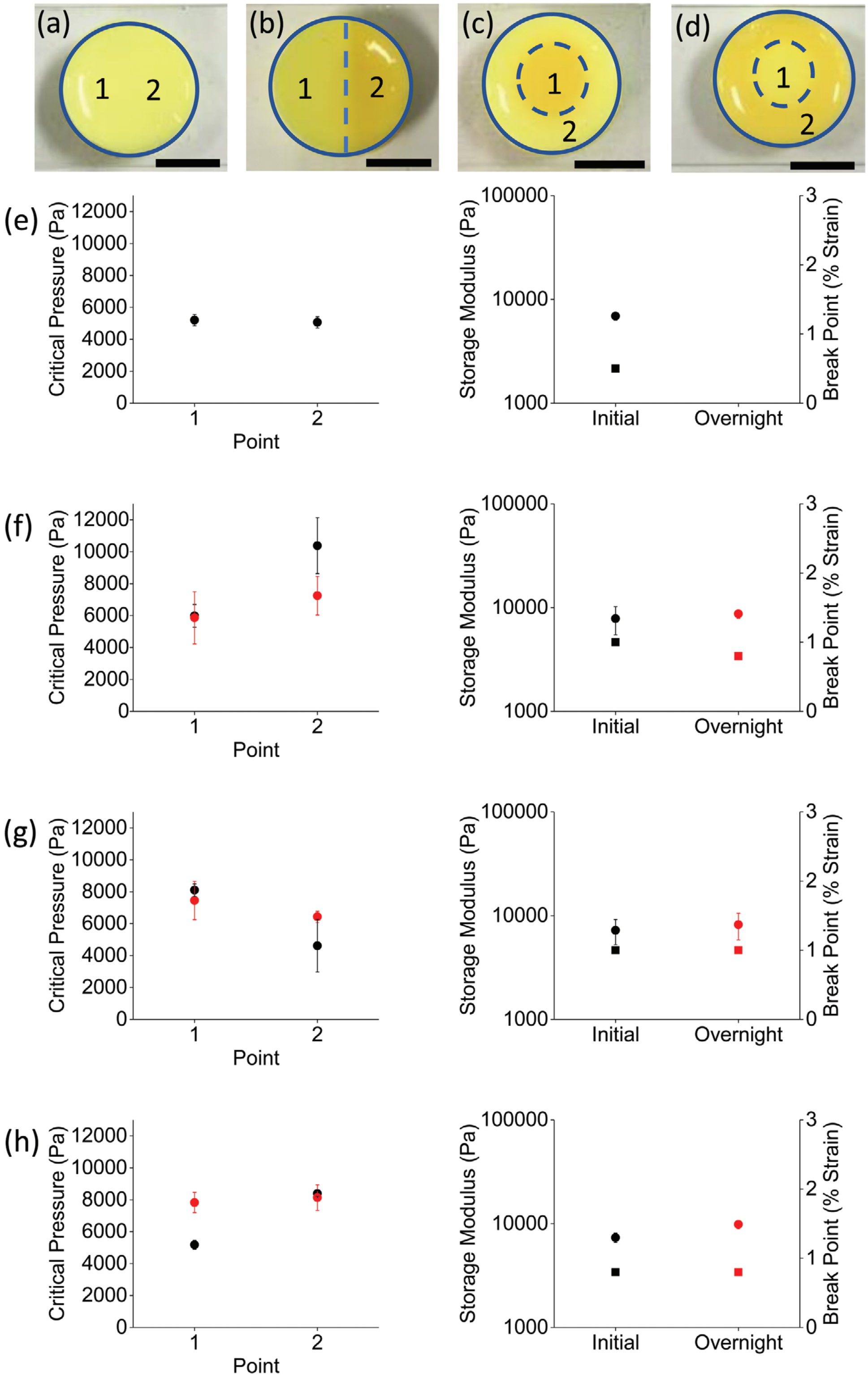

Figure 3. a–d) Photo-patterned gels formed using MBTT and GdL, showing patterns. e–h) Each photo-patterned gel was measured using cavitation (left) and bulk (right) rheology (storage modulus shown by circles, and break point shown by squares). The data in (e) corresponds to pattern (a); the data in (f) to pattern (b); the data in (g) to pattern (c); and the data in (h) to pattern (d). Black data points represent measurements taken straight after UV exposure and red data points represent measurements taken the day following UV exposure. Error bars show the standard deviation between the samples, except for break point which does not have error bars. Measurements were performed in triplicate. Scale bars represent 1 cm.

© 2020 The Authors. Published by WILEY-VCH Verlag GmbH & Co. KGaA, Weinheim

a single gelator and two pH triggers. To achieve this, we first use the minimum amount of GdL to induce gelation, tuning the amount of GdL used to form a gel, but one where the gel moduli are expected to increase significantly when the pH is further decreased (Figure S17, Supporting Information). At this point, a gel network will be formed, and we expect all 2NapFF will be assembled, but there will still be a significant degree of charge on the structures. As such, a further pH decrease results in the gel becoming stiffer.[16] Using 2.5 mg mL^{-1} of GdL results in homogeneous gels where G′ and G″ are different by an order of magnitude. We then utilize MBTT by irradiating selected regions of the soft GdL triggered gel.

To create a pattern, a photomask was used to block UV radiation to selected parts of the weak gel formed using GdL (example patterns shown in **Figure 3**). The sections not covered by the photomask were irradiated for 1 h and became darker in color. Cavitation rheology, as a localized technique, was used to probe sections of the sample at different points (points 1 and 2 in Figure 3a–d). The cavitation rheology data, Figure 3 (left), show the difference in critical pressures obtained when probing a section of irradiated and non-irradiated gel. For a control gel with no UV radiation (Figure 3e), each point measured within this pattern gave very similar critical pressure values. The final pH of these control samples was found to be 4.6. For gels where a section was irradiated, patterns (b)–(d) the sections of gel that had been irradiated gave higher critical pressure values than those covered by the mask (Figure 3f–h). This shows that the further decrease in the pH leads to the gel becoming stiffer where the gel has been irradiated. As expected from the data using MBTT alone, the pH of the samples and hence the rheology became homogeneous with time, leading to similar critical pressure values at each point after approximately 16 h (Figure 3, cavitation rheology data). All patterned samples had an average pH difference of 0.3 across the irradiated and non-irradiated sections and when left overnight, all samples were found to have the same pH throughout (Table S4, Supporting Information).

To conclude, we have shown how we can form supramolecular hydrogels with a tunable gradient of stiffness. We can create a gradual gradient when forming a gel using MBTT and also a change of stiffness within photo-patterned gels formed using a combination of GdL and MBTT. The gradients created are temporary, and when left overnight, gels become homogeneous. This is due to the diffusion of protons over time, which results in a homogenous pH and stiffness. These methods therefore allow us to prepare new types of gel and should open up opportunities in a number of areas. While we acknowledge that using the current pH range and photoinitiator may preclude biological applications, the concept could be applied using a different system. We further imagine that this concept could be used to control diffusion gradients across gels by either or both controlling pH and network gradients. This could be used to allow reactions in localized sites and the gradual diffusion of the products across the whole gel for example.

Supporting Information

Supporting Information is available from the Wiley Online Library or from the author.

Acknowledgements

L.T. thanks the University of Glasgow for funding a studentship. D.J.A. thanks the EPSRC for a Fellowship (EP/L021978/1). E.R.D. thanks the Leverhulme Trust for funding (ECF-2017-223) and the University of Glasgow for an LKAS Leadership Fellowship. The experiment at the Institut Laue-Langevin was allocated beam time under experiment number 9-11-1905 (DOI: 10.5291/ILL-DATA.9-11-1905). This work benefitted from SasView software, originally developed by the DANSE project under NSF award DMR-0520547.

Conflict of Interest

The authors declare no conflict of interest.

Keywords

dipeptide, gels, patterning, photoacids, rheology

Received: February 26, 2020
Revised: March 26, 2020
Published online: April 16, 2020

[1] N. M. Sangeetha, U. Maitra, *Chem. Soc. Rev.* **2005**, *34*, 821.
[2] a) M. de Loos, B. L. Feringa, J. H. van Esch, *Eur. J. Org. Chem.* **2005**, *2005*, 3615; b) P. J. Willcox, D. W. HowieJr., K. Schmidt-Rohr, D. A. Hoagland, S. P. Gido, S. Pudjijanto, L. W. Kleiner, S. Venkatraman, *J. Polym. Sci., Part B: Polym. Phys.* **1999**, *37*, 3438.
[3] S. Zhang, *Nat. Biotechnol.* **2003**, *21*, 1171.
[4] a) H. Kar, S. Ghosh, *Nat. Chem.* **2015**, *7*, 765; b) R. G. Weiss, *J. Am. Chem. Soc.* **2014**, *136*, 7519.
[5] a) M. Singh, C. Berkland, M. S. Detamore, *Tissue Eng., Part B* **2008**, *14*, 341; b) L. M. Cross, K. Shah, S. Palani, C. W. Peak, A. K. Gaharwar, *Nanomedicine* **2018**, *14*, 2465; c) T. H. Kim, D. B. An, S. H. Oh, M. K. Kang, H. H. Song, J. H. Lee, *Biomaterials* **2015**, *40*, 51; d) R. Sunyer, A. J. Jin, R. Nossal, D. L. Sackett, *PLoS One* **2012**, *7*, e46107; e) F. Brandl, F. Sommer, A. Goepferich, *Biomaterials* **2007**, *28*, 134.
[6] a) J. He, Y. Du, J. L. Villa-Uribe, C. Hwang, D. Li, A. Khademhosseini, *Adv. Funct. Mater.* **2010**, *20*, 131; b) P. Liu, C. Mai, K. Zhang, *Front. Chem. Sci. Eng.* **2018**, *12*, 383.
[7] a) K. Murata, M. Aoki, T. Nishi, A. Ikeda, S. Shinkai, *J. Chem. Soc., Chem. Commun.* **1991**, *24*, 1715; b) A. R. Hirst, B. Escuder, J. F. Miravet, D. K. Smith, *Angew. Chem., Int. Ed.* **2008**, *47*, 8002.
[8] a) J. A. Burdick, A. Khademhosseini, R. Langer, *Langmuir* **2004**, *20*, 5153; b) Y. Du, J. Shim, M. Vidula, M. J. Hancock, E. Lo, B. G. Chung, J. T. Borenstein, M. Khabiry, D. M. Cropek, A. Khademhosseini, *Lab Chip* **2009**, *9*, 761.
[9] J. V. Karpiak, Y. Ner, A. Almutairi, *Adv. Mater.* **2012**, *24*, 1466.
[10] I. Ziemecka, G. J. M. Koper, A. G. L. Olive, J. H. van Esch, *Soft Matter* **2013**, *9*, 1556.
[11] a) E. R. Draper, M. Wallace, R. Schweins, R. J. Poole, D. J. Adams, *Langmuir* **2017**, *33*, 2387; b) E. R. Draper, B. Dietrich, K. McAulay, C. Brasnett, H. Abdizadeh, I. Patmanidis, S. J. Marrink, H. Su, H. Cui, R. Schweins, A. Seddon, D. J. Adams, *Matter* **2020**, *2*, 764.
[12] a) Y. Pocker, E. Green, *J. Am. Chem. Soc.* **1973**, *95*, 113; b) D. J. Adams, M. F. Butler, W. J. Frith, M. Kirkland, L. Mullen, P. Sanderson, *Soft Matter* **2009**, *5*, 1856; c) T. Hu, Z. Zhang, H. Hy, S. R. Euston, S. Pan, *Biomacromolecules* **2020**, *21*, 670; d) A. D. Farahani, A. D. Martin, H. Iranmanesh, M. M. Bhadbhade,

© 2020 The Authors. Published by WILEY-VCH Verlag GmbH & Co. KGaA, Weinheim

J. E. Beves, P Thordarson, *ChemPhysChem* **2019**, *20*, 972; e) C. C. Piras, D. K. Smith, *Chem. - Eur. J.* **2019**, *25*, 11318.

[13] J. Raeburn, T. O. McDonald, D. J. Adams, *Chem. Commun.* **2012**, *48*, 9355.

[14] a) G. Pohlers, J. C. Scaiano, R. Sinta, R. Brainard, D. Pai, *Chem. Mater.* **1997**, *9*, 1353; b) J. Zhang, P. Xiao, F. Morlet-Savary, B. Graff, J. P. Fouassier, J. Lalevée, *Polym. Chem.* **2014**, *5*, 6019.

[15] a) J. A. Zimberlin, N. Sanabria-DeLong, G. N. Tew, A. J. Crosby, *Soft Matter* **2007**, *3*, 763; b) J. A. Zimberlin, J. J. McManus, A. J. Crosby, *Soft Matter* **2010**, *6*, 3632; c) A. M. Fuentes-Caparrós, B. Dietrich, L. Thomson, C. Chauveau, D. J. Adams, *Soft Matter* **2019**, *15*, 6340.

[16] L. Chen, K. Morris, A. Laybourn, D. Elias, M. R. Hicks, A. Rodger, L. Serpell, D. J. Adams, *Langmuir* **2010**, *26*, 5232.

[17] M. Wallace, J. A. Iggo, D. J. Adams, *Soft Matter* **2015**, *11*, 7739.

[18] a) E. R. Draper, E. G. B. Eden, T. O. McDonald, D. J. Adams, *Nat. Chem.* **2015**, *7*, 848; b) D. J. Cornwell, O. J. Daubney, D. K. Smith, *J. Am. Chem. Soc.* **2015**, *137*, 15486.

 © 2020 The Authors. Published by WILEY-VCH Verlag GmbH & Co. KGaA, Weinheim